

INVESTIGATION OF DIELECTRIC BEHAVIOR OF NEW Tb³⁺ DOPED BiFeO₃ NANOCRYSTALS SYNTHESIZED VIA MICRO-EMUSLION ROUTE

Z. ANWAR^a, M. AZHAR KHAN^{a*}, I. ALI^b, M. ASGHAR^a, M. SHER^c, I. SHAKIR^d, M. SARFRAZ^d, M. FAROOQ WARSI^{a*}

^a*Department of Physics, The Islamia University of Bahawalpur, Bahawalpur 63100, Pakistan*

^b*Department of Physics, Bahauddin Zakariya University, Multan 60800, Pakistan*

^c*Department of Chemistry, The University of Sargodha, Sargodha 40100, Pakistan*

^d*Deanship of Scientific Research, College of Engineering, PO Box 800, King Saud University, Riyadh 11421, Saudi Arabia*

^e*Department of Chemistry, The Islamia University of Bahawalpur, Bahawalpur 63100, Pakistan*

The effect of Tb³⁺ substitution at B site of nanoparticulate BiFeO₃ on various dielectric parameters was evaluated at room temperature in the frequency range of 1 MHz to 3 GHz. The value of x (i.e. Tb contents) was in the range of 0.00 to 0.02. Materials that have high dielectric constant cause resist the penetration of electromagnetic waves; therefore for devices working at high frequencies the low dielectric constant materials are preferred. The minimum dielectric constant (27.65) was observed at 3 GHz for Tb_{0.008}Bi_{0.992}FeO₃, however the maximum dielectric constant (87.56) was observed for Tb_{0.012}Bi_{0.88}FeO₃ at ~ 1.00 MHz. Similar trends were observed for dielectric loss and tanδ values. In general for all compositions usually low dielectric constant, dielectric loss and tanδ were observed that suggest the applications of these materials for fabrications of devices that are required to operate at higher (GHz) frequencies range. Besides main types of dielectric parameters, the other parameters related to dielectric behavior such as ac-conductivity (σ_{ac}), the electrical modulus (M) etc were also evaluated. The ac-conductivity was found to increase with increased frequency and the maximum ac-conductivity was observed for Tb_{0.012}Bi_{0.88}FeO₃ nanoparticles. The mechanism of charge transport processes by electrical transport; ion dynamics and conductivity relaxation have also been explained in detail.

(Received October 11, 2014; Accepted December 5, 2014)

Keywords: Chemical synthesis; Nanostructures; Dielectric properties

1. Introduction

Dielectric materials are technological very important and have a wide range of applications [1]. The desired materials with required dielectric properties can be obtained by controlling various factors such as judicious choice of the metals, their stoichiometric ratio, method of preparation, size control of the particles etc [2, 3]. For example they are usually high resistive materials such as ferrites and are used as resonators in telecommunication devices, microwave absorbers, magnetic data storage etc [4, 5]. From chemistry point of view, the dielectric materials are usually oxides of various metals (transition metals and rare earths). The main reason of their utilization at higher frequencies (micro-wave region) is inherent large built in “biasing field” [6]. Ferrites and perovskites are two important classes of metal oxides. Ferrites are magnetic (soft or hard magnets depending upon the Fe contents) in nature and also have high resistivity (i.e. low

*Corresponding author: azhar.khan@iub.edu.pk

dielectric constant). Ferrites are good dielectric materials and have been extensively investigated [1, 6-9]. Perovskites is class of metal oxides with general formula ABO_3 (Where A and B are divalent and trivalent metal ions respectively). The perovskites have also diverse applications such as cathode material in solid oxide fuel cells, catalytic applications, and can also be magnetic in nature depending upon the presence of iron contents. For example $BiFeO_3$ is a well known multiferroic materials and is under extensive study for various applications like in spintronics, structural variation by metal ion substitution etc [10]. Ahmad et al. recently studied the effect of Al-Mn doping at Fe-site of $BiFeO_3$ They showed successful double ion substitution successfully by co-precipitation route [11]. Similarly the effects of doping of various rare earths in $BiFeO_3$ also have been reported [12-16].

To the best of our knowledge, the dielectric behavior of nanoparticulate Tb-doped $BiFeO_3$ has not been explored in detail. Here in this article, we aim to investigate the effect of Tb^{3+} in $BiFeO_3$ on various dielectric parameters and to explore the possible utilization of these nanomaterials in microwave devices applications.

2. Materials and Methods

The Tb-doped $BiFeO_3$ nanoparticles prepared by micro-emulsion route and were characterized by thermogravimetric analysis, X-ray diffraction, scanning electron microscopy etc. The synthesis and characterization of Tb-doped $BiFeO_3$ nanoparticles has been described in detail in our previous communication [17].

3. Results and Discussion

3.1 Dielectric Properties

The relative speed that an electromagnetic signal can travel in a material is determined by the dielectric constant of that material. The speed of microwaves decreases by a factor nearly equal to the square root of the dielectric constant, when microwaves enter in a dielectric material [18]. Fig.1 shows the variation of dielectric constant as a function of frequency from MHz to 3 GHz range. There is a gradual decrease in dielectric constant with few resonance peaks observed at higher frequencies. Dipoles relaxation is responsible for dispersion in dielectric constant at lower frequency; however the matching of the applied field frequency and the frequency of charge transfer between Fe^{2+} and Fe^{3+} can produce resonance at higher frequencies [19].

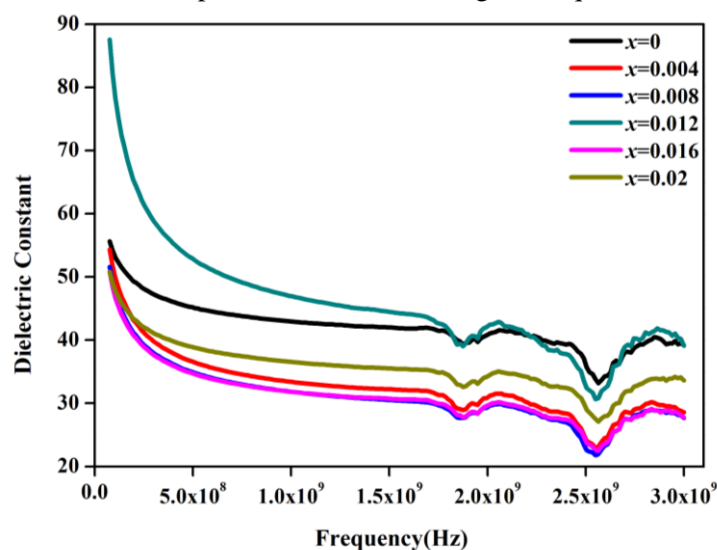


Fig. 1. Dielectric constant as a function of frequency

Non-uniform distribution of oxygen ions at grains and grain boundaries during sintering results in interfacial polarization at lower frequencies, however at high frequencies dipolar, ionic, electronic polarization respectively contributes to dielectric constant [6]. Polarization reduces the field inside the medium; hence dielectric constant decreases by increase in frequency [20]. Dipolar and ionic polarizations are the dominating mechanisms contributing to dielectric properties in radio (MHz) to microwave (GHz) frequency range. In real materials, at micro-wave frequency and beyond, resonance peaks are observed due to un-damped dipoles. However strongly damped dispersions are observed below microwave frequency [21]. The variation of dielectric constant with frequency can be explained on the basis of space charge polarization which is produced due to the presence of high conductivity phases (grains) separated from low conductivity matrix (grain boundaries) in a dielectric medium [22]. The assembly of space charge carriers in a dielectric takes a finite time to line up their axes parallel to an alternating field. If the frequency of the field reversal increases, a point is reached where the space charge carriers cannot keep up with the applied field and the alternation of their direction lags behind that of the field applied [23] and hence results in the decrease of dielectric constant of a material. According to Iwachi large number of Fe^{2+} ions at octahedral sites increases the electronic transfer between Fe^{2+} and Fe^{3+} and results in higher values of dielectric constant [5]. In Koops model for heterogeneous dielectrics the reason for the dispersion in the dielectric constant is that the electrons can respond to the changes in applied electric field only if the time required for hopping is less than half the period of the alternating field [18]. High dielectric constant decreases the penetration depth of the electromagnetic waves by increasing the skin effect. Hence, the much lower dielectric constants obtained for the present samples make them suitable for their applications at high frequency [7]. These samples may attenuate the unwanted interference greater than 1GHz.

Fig. 2 shows the behavior of dielectric loss as a function of increasing frequency which is quite similar to real part of the dielectric constant that can be explained according to Smith and Wijn that there is an inverse relation between the ratio of complex dielectric permittivity to ac conductivity with the applied field [24]. Materials having high conductivity generally have high dielectric losses and vice versa [25, 26].

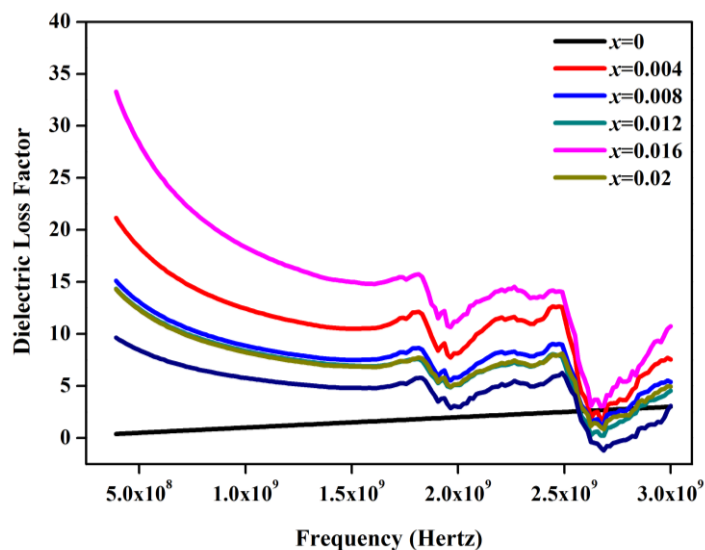


Fig. 2: Dielectric loss as a function of frequency

Fig.3 indicates the variation in dielectric loss tangent with frequency. Several factors affect the value of $\tan\delta$ such as stoichiometry, structural homogeneity, which in turn depend on composition and sintering temperature of the samples [27]. According to Maxwell–Wagner theory both ϵ' and $\tan\delta$ are inversely proportional with frequency [2]. Low dielectric losses are required for low core loss and energy dissipation in the dielectric system is represented by Dielectric loss

factor ($\tan \delta$) [28]. Peak in the graph appear because of the strong correlation between conduction and the dielectric behavior in these samples.

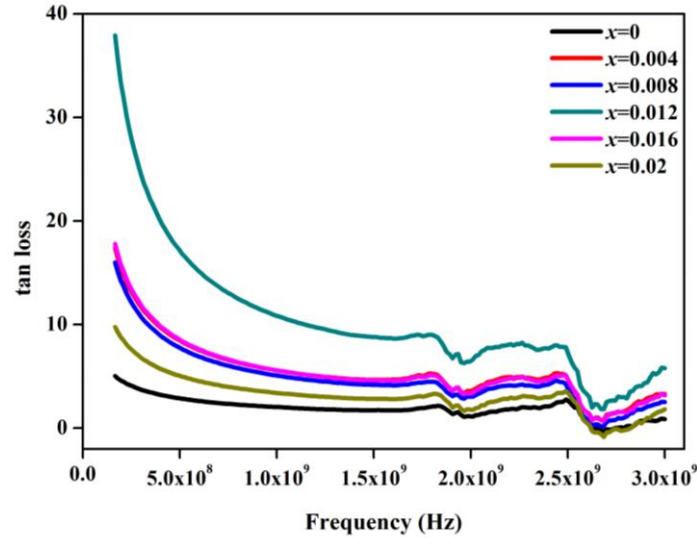


Fig. 3. Dielectric loss tangent as a function of frequency

3.2 AC-Conductivity

AC conductivity can be written as the sum of two components as follows;

$$\sigma_{ac} = \sigma_1(T) + \sigma_2(\omega, T) \quad (1)$$

Where the first term is the DC part of the electrical conductivity and the second term $\sigma_2(\omega, T)$ is frequency and temperature dependent and related to the dielectric relaxation caused by bound or localized electric charge carriers. It obeys a power law which could be written as [29].

$$\sigma_2(\omega, T) = B(T) \omega^{n(T)} \quad (2)$$

Where $\omega = 2\pi f$ is the angular frequency, B is temperature dependent parameter and has conductivity units $(\Omega\text{-cm})^{-1}$. The exponent parameter “n” is a non-dimensional temperature dependent parameter with values between 0 and 1 [30]. Fig.4 shows the behavior of $\ln\sigma_{ac}$ with $\ln\omega$. The ac-conductivity of the present samples was calculated using the relation

$$\sigma_{ac} = \omega \epsilon_0 \epsilon'' \quad (3)$$

Where $\omega = 2\pi f$ and ϵ'' is the dielectric loss. It can be observed from Fig.4 that conductivity increases with increase in frequency.

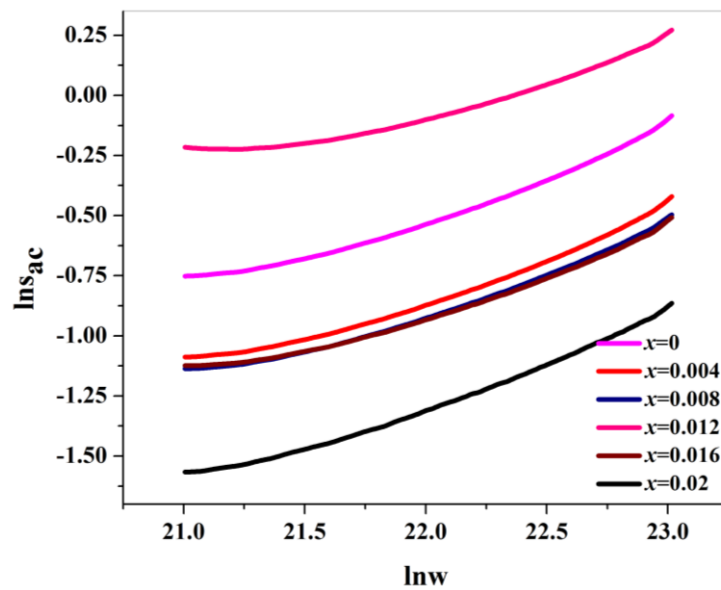


Fig. 4: Relation between $\ln\omega$ and $\ln\sigma_{ac}$

Since the increase in frequency enhances the hopping frequency of the charge carriers between Fe^{2+} and Fe^{3+} , the conductivity increases. Heterogeneous Model of polycrystalline structure can be used to explain this behavior. According to this Model polycrystalline materials consist of conducting grains separated by highly resistive thin layers (grain boundaries). Our results of ac conductivity at low frequencies describe the grain boundary behavior, while the dispersion at high frequency may be attributed to the conductivity of grains [9]. The exponent ‘n’ was calculated as a function of composition by plotting $\ln(\sigma)$ versus $\ln(\omega)$ according to the equation.

$$\sigma(\omega) = B\omega^n \quad (4)$$

which represents the straight lines with slope equal to exponent ‘n’ and intercept equal to $\ln B$ on vertical axis at $\ln\omega = 0$. It is clearly shown in Fig.5 that the value of ‘n’ lies between 0 and 1. When $n = 0$, the electrical conduction is frequency independent and for $n \leq 1$, the conduction is frequency dependent [8]. In the present study, the value of exponent varies between 0.27-0.37, which suggests that the conduction phenomena in the present samples follow hopping conduction.

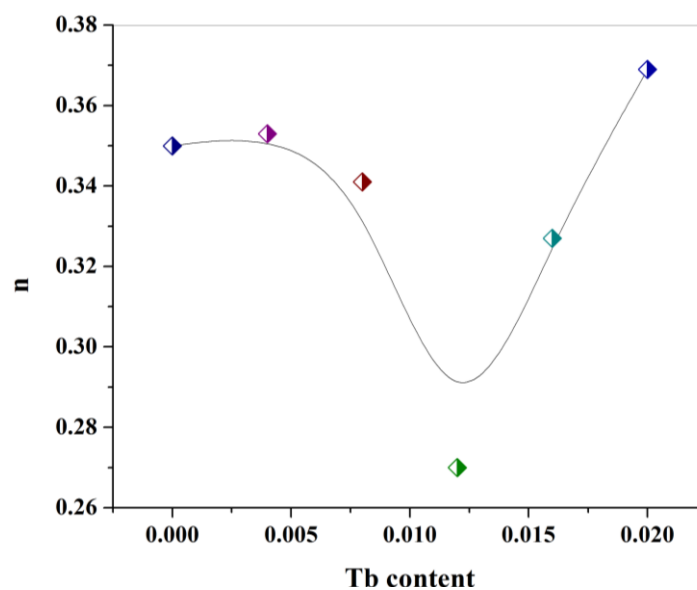


Fig. 5: n as function of Tb substitution

3.3 Cole–Cole plots

To separate the grain and grain boundary contributions, complex impedance plane plots (Cole–Cole plots) have been investigated. The nano crystalline samples are characterized by small grain size and large number of grain boundaries. The electrical modulus (M) was used, in order to study the frequency dependences of the interfacial polarization effect, which generates electric charge accumulation around the ceramic particles by displacing relaxation peaks. The Maxwell–Wagner model provides to assess the behavior of complex conductivity in heterogeneous systems having two or more phases [31].

In a heterogeneous system, if the region of grain boundary occupies a large volume, the graph of the modulus ($M^* = 1/\epsilon^*$) M'' versus M' provides better information about the semi circles. It suggests that there is a probable relationship between the behavior of grain boundary and the appearance of the peaks of M'' as a function of frequency. In the second case, if the region of continuity of the grain boundary occupies a small volume, the spectrum of impedance (Z'' versus Z') provides better visualization of the semi circles in the plane. Since there is a probable relationship between the behavior of grain boundary and the appearance of the peaks in M'' as a function of frequency, former case is in great agreement with our present experimental results. The complex impedance (Cole–Cole) plots using M' and M'' as two variants are plotted in Fig.6. A semi-circle was obtained for all the samples. It was observed from these plots that the major contribution in the conduction is due to grain boundary density. At lower frequency i.e. left side of the semi-circle is a result of grain resistance [4], while the intermediate frequencies represent grain boundary contribution [32]. Taking into account the higher frequency region, extreme right side represents the whole resistance of both grain and grain boundaries [4].

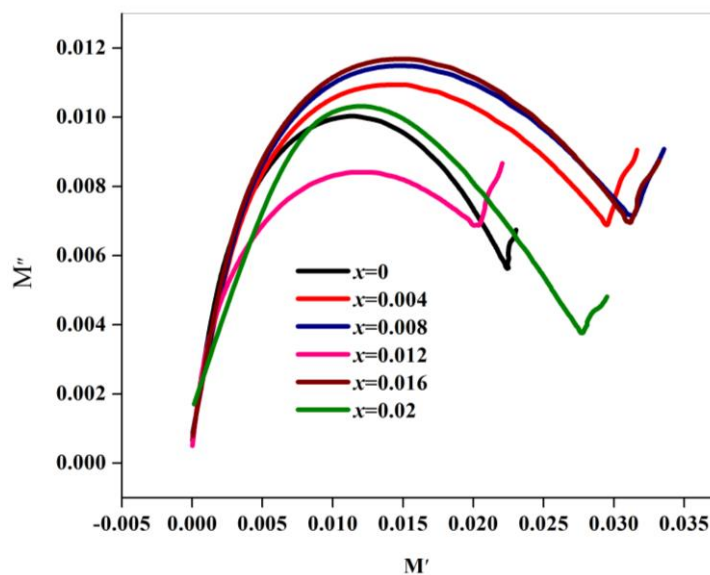


Fig. 6: Cole-Cole plot of Tb substituted BiFeO_3

Addition of Tb^{3+} enhances the grain boundaries density which in turn leads to a remarkable rise of grain boundary resistance. Therefore, the conduction mechanism, observed in complex impedance measurement, is well in agreement with the AC conductivity phenomenon, reported earlier. However, as compared to the grain contribution, only grain boundary contribution is clearly observed from Cole–Cole plots.

The variation of real part of electric modulus (M') as a function of frequency is shown in Fig.7.

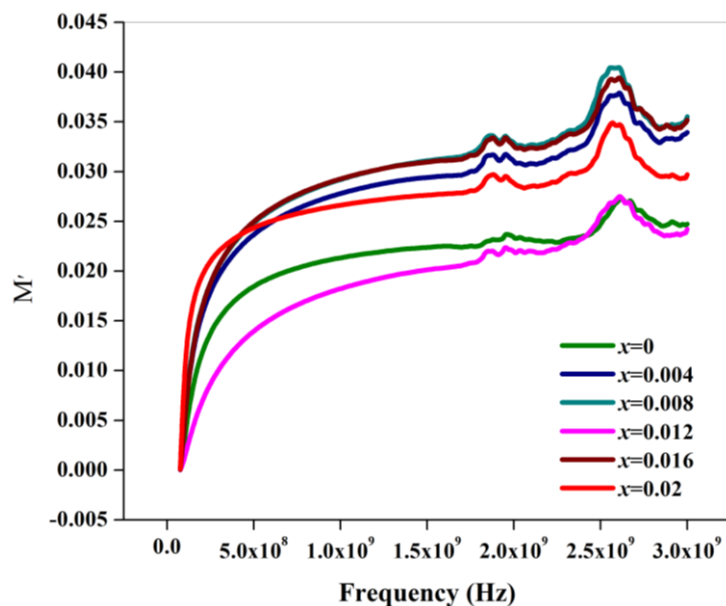


Fig. 7. Real part of modulus as a function of frequency

The value of M' is very low in the low frequency region. As frequency increases the value of M' increases and reaches a maximum constant value of $M_{\infty}=1/\epsilon_{\infty}$ at higher frequencies for all samples. These observations may possibly be related to a lack of restoring force governing the mobility of charge carriers under the action of an induced electric field. These features indicate that the electrode polarization makes a negligible contribution in the material [33]. This type of behavior supports the conduction phenomena due to long-range mobility of charge carriers.

The frequency dependence of the imaginary part of the electric modulus (M'') exhibits a maximum in Fig.8. This pattern provides wider information relating charge transport processes such as mechanism of electrical transport, conductivity relaxation, and ion dynamics as a function of frequency. The frequency region below the peak maximum determines the range in which charge carriers are mobile over long distances. At the frequency above peak maximum (high-frequency), the carriers are confined to potential wells, being mobile over short distances. Their region where the peak occurs is indicative of the transition from long-range to short-range mobility with increase in frequency. Further, the appearance of peak in the modulus spectrum provides a clear indication of conductivity relaxation [34]. The condition for observing maxima in (M'') of a material is [35].

$$\omega \tau = 1 \quad (5)$$

Where $\omega=2\pi f_{max}$ and τ is relaxation time.

Now, the relaxation time is related to jumping probability per unit time P by relation

$$\tau = (1/2) P \text{ or } f_{max} \propto P \quad (6)$$

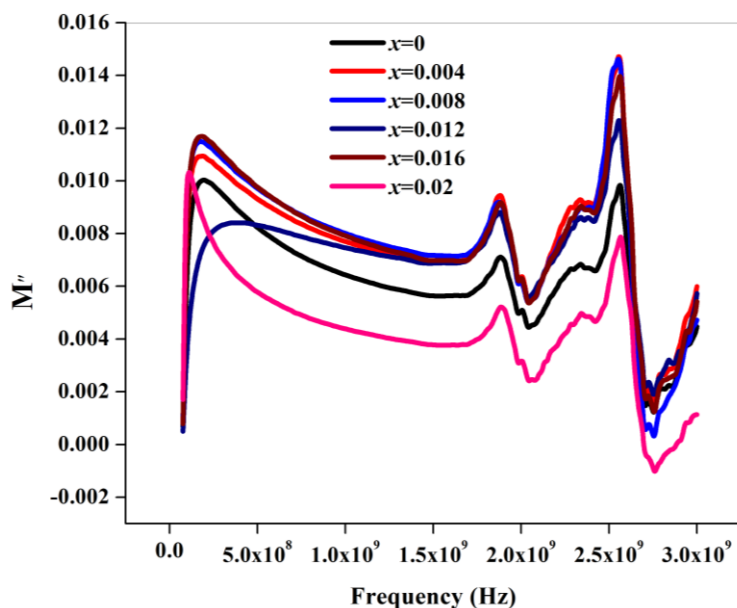


Fig. 8. Imaginary part of modulus as a function of frequency

4. Conclusion

Various dielectric and related parameters such as dielectric constant, dielectric loss, $\tan\delta$, ac-conductivity and electric modulus were evaluated for $\text{Tb}_x\text{Bi}_x\text{FeO}_3$ ($x = 0.00$ to 0.02) in the frequency range 1.0 MHz to 3.0 GHz. Overall low dielectric parameters were obtained, that suggest the potential utilization of these materials for fabricating the devices that operate in GHz frequencies. The phenomenon of charge transport by conductivity relaxation, ion dynamics and electrical transport has been greatly influenced by the Tb incorporation.

Acknowledgement

The authors (I. Shakir & M. Sarfraz) are thankful to the Deanship of Scientific Research, King Saud University for the funding through research group project no. RGP-VPP-312.

References

- [1] M.Y. Lodhi, K. Mahmood, A. Mahmood, H. Malik, M.F. Warsi, I. Shakir, M. Asghar, M.A. Khan, *Current Applied Physics*, **14**, 716 (2014).
- [2] R. Peelamedu, C. Grimes, D. Agrawal, R. Roy, *Journal of Materials Research* **18**, 2292 (2003).
- [3] H. Malik, A. Mahmood, K. Mahmood, M.Y. Lodhi, M.F. Warsi, I. Shakir, H. Wahab, M. Asghar, M.A. Khan, *Ceramics International*, **40**, 9439 (2014).
- [4] Y. Bai, J. Zhou, Z. Gui, L. Li, *Journal of Magnetism and Magnetic Materials* **278**, 208 (2004).
- [5] M.J. Iqbal, M.N. Ashiq, P. Hernandez-Gomez, J.M. Munoz, *Journal of Magnetism and Magnetic Materials*, **320**, 881 (2008).
- [6] S.B. Narang, I.S. Hudiara, *Journal of Ceramic Processing Research*, **7**, 113 (2006).
- [7] M.J. Iqbal, M.N. Ashiq, *Chemical Engineering Journal*, **136**, 383 (2008).
- [8] M. Irfan, M.U. Islam, I. Ali, M.A. Iqbal, N. Karamat, H.M. Khan, *Current Applied Physics*, **14**, 112 (2014).
- [9] S. Hussain, A. Maqsood, *Journal of Alloys and Compounds*, **466**, 293 (2008).
- [10] B. Kundys, M. Viret, D. Colson, D.O. Kundys, *Nat Mater*, **9**, 803 (2010).
- [11] B. Ahmad, A. Mahmood, M.N. Ashiq, M.A. Malana, M. Najam-UI-Haq, M.F. Ehsan,

- M.F. Warsi, I. Shakir, *Journal of Alloys and Compounds*, **590**, 193 (2014).
- [12] G.S. Lotey, N.K. Verma, *Superlattices and Microstructures*, **60**, 60 (2013).
- [13] G.S. Lotey, N.K. Verma, *Superlattices and Microstructures*, **53**, 184 (2013).
- [14] Q. Zhang, X. Zhu, Y. Xu, H. Gao, Y. Xiao, D. Liang, J. Zhu, J. Zhu, D. Xiao, *Journal of Alloys and Compounds*, **546**, 57 (2013).
- [15] T.D. Rao, T. Karthik, S. Asthana, *Journal of Rare Earths*, **31**, 370 (2013).
- [16] L. Zhang, Y. Yang, S. Ma, W. Luo, Y. Liu, K. Zhu, *Physica B: Condensed Matter* **407**, 494 (2012).
- [17] Z. Anwar, M. Azhar Khan, A. Mahmood, M. Asghar, I. Shakir, M. Shahid, I. Bibi, M. Farooq Warsi, *Journal of Magnetism and Magnetic Materials*, **355**, 169 (2014).
- [18] M. Anis-ur-Rehman, G. Asghar, *Journal of Alloys and Compounds*, **509**, 435 (2011).
- [19] S.V. J. Chand, P.Kumar, M. Singh, , *Journal of Theoretical and Applied Science* **3**, 8 (2011).
- [20] S.F. Mansour, *Egyptian Journal of Solids* **2**, 263 (2005).
- [21] P.J. Harrop, *Dielectrics*, Butterworths, London, 1972, (1972).
- [22] M. Chanda, *Science of Engineering Materials*, The Machmillan Company of India Ltd., New Delhi 3 (1980).
- [23] A.M. Shaikh, S.S. Bellad, B.K. Chougule, *Journal of Magnetism and Magnetic Materials*, **195**, 384 (1999).
- [24] G.F.M. Pires Júnior, H.O. Rodrigues, J.S. Almeida, E.O. Sancho, J.C. Góes, M.M. Costa, J.C. Denardin, A.S.B. Sombra, *Journal of Alloys and Compounds*, **493**, 326 (2010).
- [25] M.N. Ashiq, M.J. Iqbal, I.H. Gul, *Journal of Alloys and Compounds*, **487**, 341 (2009).
- [26] I.H. Gul, A. Maqsood, *Journal of Alloys and Compounds*, **465**, 227 (2008).
- [27] M.N. Ashiq, M. Javed Iqbal, I. Hussain Gul, *Journal of Magnetism and Magnetic Materials*, **323**, 259 (2011).
- [28] M. Javed Iqbal, M. Naeem Ashiq, I. Hussain Gul, *Journal of Magnetism and Magnetic Materials*, **322**, 1720 (2010).
- [29] M.A. El Hiti, *Journal of Magnetism and Magnetic Materials*, **164**, 187 (1996).
- [30] A.M. Abo El Ata, M.K. El Nimr, S.M. Attia, D. El Kony, A.H. Al-Hammadi, *Journal of Magnetism and Magnetic Materials*, **297**, 33 (2006).
- [31] H.O. Rodrigues, G.F.M. Pires Junior, A.J.M. Sales, P.M.O. Silva, B.F.O. Costa, P. Alcantara Jr, S.G.C. Moreira, A.S.B. Sombra, *Physica B: Condensed Matter*, **406**, 2532 (2011).
- [32] M.G. Chourashiya, J.Y. Patil, S.H. Pawar, L.D. Jadhav, *Materials Chemistry and Physics*, **109**, 39 (2008).
- [33] B.V.R. Chowdari, R. Gopalakrishnan, *Solid State Ionics*, **23**, 225 (1987).
- [34] M.M. Costa, G.F.M. Pires Júnior, A.S.B. Sombra, *Materials Chemistry and Physics*, **123**, 35 (2010).
- [35] S.M. Patange, S.E. Shirsath, K.S. Lohar, S.S. Jadhav, N. Kulkarni, K.M. Jadhav, *Physica B: Condensed Matter*, **406**, 663 (2011).